ISBN: 978-3-95450-261-5 ISSN: 2673-7000 doi: 10.18429/JACoW-NAPAC2025-THYN01

HOW NITROGEN AND OXYGEN SHAPE SRF CAVITY PERFORMANCE*

H. Hu†[1], Y.-K. Kim[1,2], D. Bafia[2]
[1]University of Chicago, Chicago, IL, USA
[2]Fermi National Accelerator Laboratory, Batavia, IL, USA

Abstract

Nitrogen and oxygen-based surface treatments have enabled superconducting radiofrequency (SRF) cavities to reach higher gradients and lower losses. However, the exact mechanisms by which these treatments improve cavity performance remain largely unknown. This work provides new insights into the role of nitrogen and oxygen in SRF cavity performance by using time-of-flight secondary ion mass spectrometry (ToF-SIMS) to quantify the concentrations and depth profiles of nitrogen and oxygen impurities within niobium cutouts. This work correlates these impurity profiles with cavity performance measurements, including surface resistance and quality factor. The results demonstrate that while both nitrogen and oxygen enhance performance, ten times more oxygen is required to achieve the same reduction in BCS resistance as nitrogen.

INTRODUCTION

Improving the performance of superconducting radiofrequency (SRF) cavities is the key to enabling the next generation of particle accelerators such as the International Linear Collider (ILC) or the 8 GeV Booster Replacement Linac at Fermilab [1,2]. Two key performance metrics are quality factor (Q_0) and accelerating gradient (E_{acc}). Higher Q_0 cavities will lower operating costs and helium expenses [3]. High E_{acc} cavities make accelerators more efficient per unit length and enable future accelerators to reach higher energies.

The performance of the SRF cavity depends primarily on the composition of the first 100 nm of the surface, defined by the penetration length of superconducting currents [4]. The presence of free hydrogen in the surface has long been a limiting factor for high performance SRF cavities [5, 6]. At superconducting temperatures, free hydrogen dissolved within the Nb lattice will precipitate and form highly lossy niobium hydrides [7]. Many studies have been conducted on the development of surface treatments to minimize these prohibitive effects through the introduction and diffusion of impurities such as oxygen and nitrogen [8–11].

The state-of-the-art high Q_0 treatment of nitrogen doping introduces uniform and dilute concentrations of nitrogen into the surface [8]. A key performance feature of a N doped cavity is the anti Q-slope, an increase in Q_0 with increasing E_{acc}, which typically occurs at E_{acc} below 20 MV/m [8]. While there are some theories which propose the cause of anti-Q slope, there is no general consensus on which underlying mechanisms are responsible for it [12–15]. One theory is that nitrogen impurities act as a trap for interstitial hydrogen, reducing the concentration of free hydrogen and the losses from niobium hydrides [16].

The presence of interstitial oxygen in the Nb lattice has also been shown to have a similar effect as nitrogen [16]. Recent work has highlighted the role of diffused oxygen in improved SRF cavity performance [17–19]. A new surface treatment termed oxygen doping (200°C × 20 hours of *in-situ* baking) displays high Q_0 performance by introducing an approximately uniform concentration of oxygen in the surface without completely removing the oxide [17]. O doped cavities exhibit anti-Q slope, a feature previously considered to be unique to N doped cavities [20, 21]. Given the similarities in performance, it has been proposed that impurities in the surface layer of N and O doped cavities perform similar functions in mitigating sources of loss [16, 22]. First principle calculations suggest that it is energetically favorable H to bond with O and N interstitials instead of with Nb [16]. In this work, we correlate material studies with cavity studies to quantify the effect of interstitial O and N on SRF cavity performance and better understand the underlying mechanisms that drive .

EXPERIMENTAL METHOD

We prepared an array of single-cell TESLA shaped 1.3 GHz Nb cavities and Nb cavity cutouts from cavity TE1AES008 with a standardized EP baseline treatment of 120 µm electropolishing (EP) removal, 800°C degassing for 3 hours in an ultra high vacuum (UHV) furnace, and 40 µm EP removal. We then applied the treatments described in Table 1 to each corresponding cavity and cutout sample. One set of treatments consisted of *in-situ* baking at 120°C and 200°C at various durations. *In-situ* baked cavities were assembled prior to baking, and vacuum was maintained throughout the baking and testing. EP and N doped cavities were assembled post-treatment. The specific procedures for N doping treatments are described in Ref. [8]. To ensure a one-to-one comparison of the cutout surface to the inner surface of a cavity, we baked cutouts *in-situ* and maintained vacuum to avoid the regrowth of the native niobium oxide and minimize chances of contamination.

We analyzed cutouts with time-of-flight secondary ion mass spectrometry (ToF-SIMS) to obtain depth profiles of the impurities present in the Nb lattice. Each reported impurity depth profile is taken as the average of three 200 µm × 200 µm spots on each sample. The sputter crater

* This manuscript has been authored by the FermiForward Discovery Group, LLC under contract No. 89243024CSC000002 with the U.S. Department of Energy, Office of Science, Office of High Energy Physics. This work was supported by the University of Chicago.
† hannahhu@uchicago.edu

ISBN: 978-3-95450-261-5 ISSN: 2673-7000 doi: 10.18429/JACoW-NAPAC2025-THYN01

Table 1: Treatment Process History for Cavity Cutouts and 1.3 GHz Single-cell SRF Cavities

Cavity	Treatment Steps	
TE1AES010	EP Baseline	
TE1AES010	120°C × 3 hr *in-situ*	+ 120°C × 3 hr (total 6 hr) *in-situ*
TE1PAV009	120°C × 48 hr *in-situ*	
TE1AES017	200°C × 1 hr *in-situ*	+ 200°C × 10 hr (total 11 hr) *in-situ*
TE1AES021	200°C × 20 hr *in-situ*	
TE1AES024	2/0 + 5 µm N Doping	
TE1RI003	3/60 + 10 µm N Doping	

for each spot is 600 µm × 600 µm to avoid edge effects from sputterring, and the sputtering energy of the Cs ion beam is 2 keV. Vacuum was maintained at $< 4 \times 10^{-10}$ mbar in the analysis chamber and 10^{-7} mbar in the heating chamber. Cutouts were analyzed alongside implanted N and O standards to calibrate relative SIMS intensity and get the absolute concentration of N and O [23]. O^- and NbN^- signals were used to determine the relative sensitivity factor (RSF) for O and N respectively. Experimentally determined RSF values relative to the Nb were found to be 3.66×10^{21} ions/cm^3 for N and 2.11×10^{20} ions/cm^3 for O. Data from areas with particle contaminants were excluded to be representative of a clean cavity surface.

We measured cavity performance after each treatment at the Fermilab Vertical Test Stand (VTS). Cooling followed the fast cooldown protocol to minimize losses from trapping magnetic flux [17]. Power balance measurements were performed in continuous wave operation to acquire Q_0 vs. E_{acc} curves at 2 K and <1.5 K [17]. Q_0 is defined as:

$$Q_0(E_{\mathrm{acc}}, T) = \frac{G}{R_{\mathrm{res}}(E_{\mathrm{acc}}) + R_{BCS}(E_{\mathrm{acc}}, T)} \qquad (1)$$

where $G = 270\ n\Omega$ is a geometry factor determined by the shape of the cavity, T is the cavity temperature, R_{res} is residual resistance, and R_{BCS} is the BCS surface resistance [3]. We measure Q_0 vs. E_{acc} at both 2 K and <1.5 K to decompose the surface resistance and distinguish between different sources of loss. At <1.5 K, the only source of loss is R_{res}, which encompasses losses from vacancies in the niobium oxide and trapped magnetic flux, among others. At 2 K, there are contributions from both R_{res} and temperature dependent R_{BCS}. R_{BCS} describes losses introduced by quasiparticles from the breaking of superconducting Cooper pairs due to thermal excitation or photon absorption. In this work, we are interested in how the concentrations of interstitials within the Nb metal are affecting performance, so we focus on R_{BCS}.

RESULTS AND DISCUSSION

Figure 1 contains the absolute concentration of O and N measured from cavity cutouts for each of the treatments described in Table 1. An EP baseline represents a clean Nb surface in which there is only oxygen in the native niobium oxide at the surface. *In-situ* baking at 120°C gradually dissolves oxygen from this niobium oxide into the metal with a diffusion length of 40–100 nm [17]. For 200°C *in-situ* baking, the oxygen concentration is approximately uniform in the first 100 nm. The diffusion lengths are 300–1200 nm for the durations considered in this work. For N doping treatments, we observe that there is a dilute and uniform concentration of N which extends 20–30 µm into the bulk.

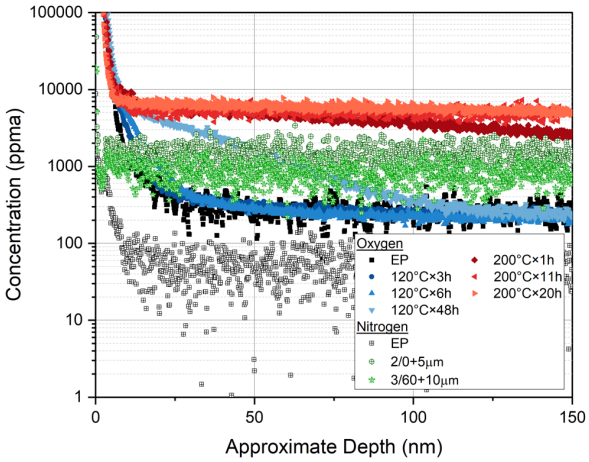

Figure 1: SIMS depth profile for absolute concentrations of N and O in Nb cavity cutouts for each treatment.

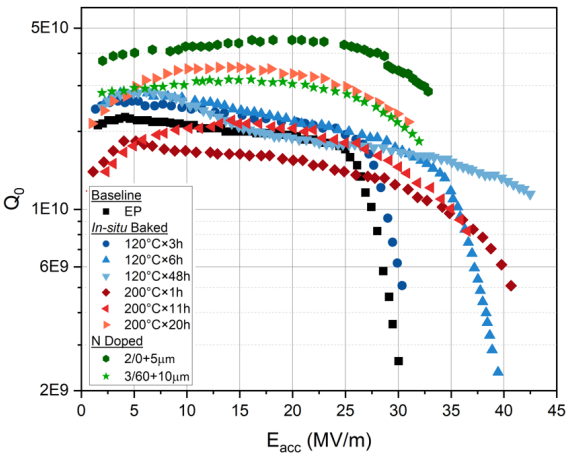

Figure 2: Q_0(2K) vs. E_{acc} performance for single-cell 1.3 GHz SRF cavities of various treatment recipes.

Figure 2 shows the Q_0 vs. E_{acc} performance at 2 K for each treatment recipe. We observe that EP displays high field Q-slope (HFQS), a phenomena where Q_0 rapidly degrades at higher fields [10]. The onset of HFQS can be gradually

ISBN: 978-3-95450-261-5 ISSN: 2673-7000 doi: 10.18429/JACoW-NAPAC2025-THYN01

extended to higher fields with increased 120°C baking. This has enabled 120°C baked cavities to reach high E_{acc} above 40 MV/m. Sequential baking at 200°C and N doping appears to enhance Q_0 rather than E_{acc}. We note that baking at 200°C × 20 hours and a 3/60 + 10 µm N doping treatment yield remarkably similar performance. One such performance feature is the anti-Q slope at low fields which has enabled these treatments to reach high Q_0.

Decomposed BCS surface resistance curves with field for each of these treatments are plotted in Fig. 3. Increased baking duration and higher baking temperatures lead to lower R_{BCS}. Decreases in R_{BCS} appear to be driving the improvements in Q_0 observed in Fig. 2. Anti-Q slope arises from a decrease in R_{BCS} with field. 200°C × 20 hours and the N doped treatments display similarly low R_{BCS} of about 5.5 nΩ.

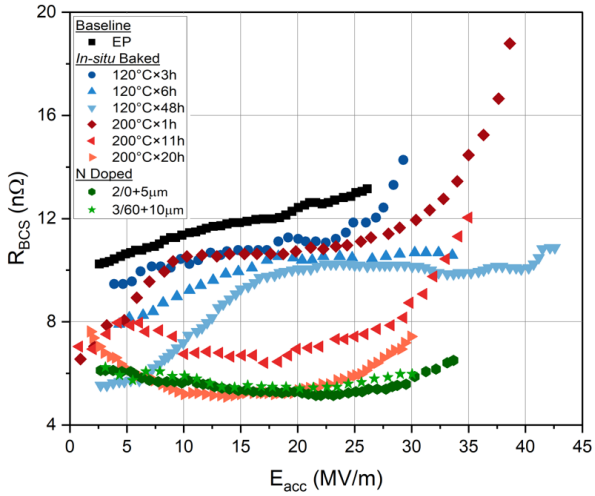

Figure 3: R_{BCS}(2K) vs. E_{acc} performance for various treatment recipes.

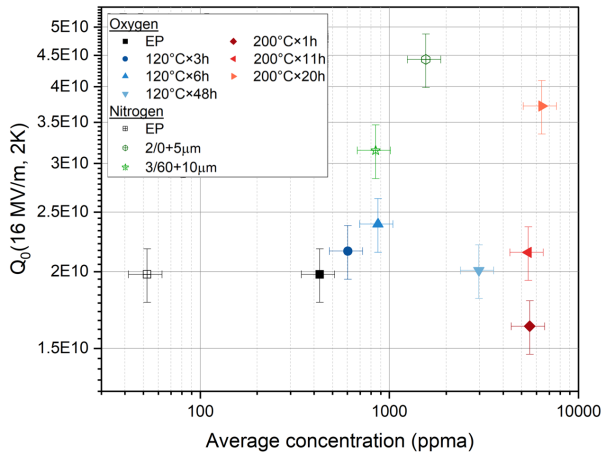

Figure 4: Q_0(16 MV/m) vs. the average absolute concentration of N and O.

We summarize the data from Fig. 1 by averaging over the concentration of impurities in the first 100 nm of the surface. We exclude contributions from the first 15 nm due to the presence of the native niobium oxide. From Figs. 2 and 3, we extracted Q_0 and R_{BCS} at 16 MV/m for each of the treatments. 16 MV/m was chosen as it avoids both high field Q-slope degradation at >25 MV/m and low field (<5 MV/m) effects from surface oxides. We correlate the average concentrations with Q_0(16 MV/m, 2K) and R_{BCS}(16 MV/m, 2K) in Figs. 4 and 5.

Figure 4 plots Q_0(16 MV/m, 2K) against the average concentrations of O and N. We do not observe any distinguishable trends in performance with concentration since Q_0 is sensitive to both changes in the native oxide and in the metal. Focusing on just the losses in the metal, we show changes in R_{BCS} with concentration in Fig. 5. From a baseline R_{BCS} of 12 nΩ for EP, R_{BCS} decreases as more O is diffused into the Nb bulk. A similar trend is observed for nitrogen, but with significantly less diffused N. Namely, we can achieve the same reduction in R_{BCS} with an order of magnitude less of N interstitials compared to O interstitials. Microscopically, this suggests that N is much more effective at trapping H than O.

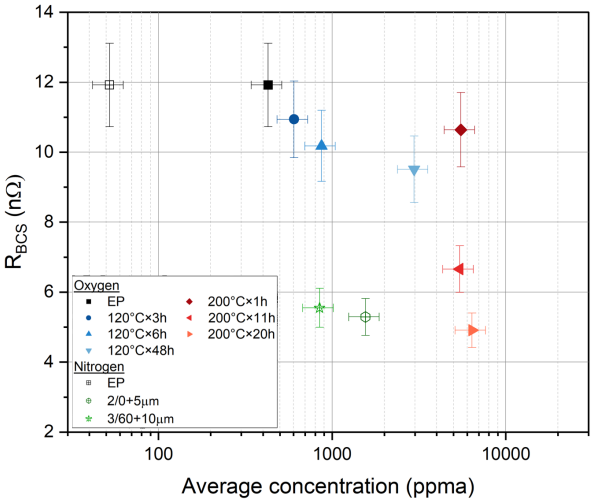

Figure 5: R_{BCS}(16 MV/m, 2 K) vs. the average absolute concentration of N and O.

CONCLUSION

We performed material and cavity performance measurements on a number of SRF treatment recipes. We correlated the absolute concentration of O and N in cavity cutouts with Q_0 and R_{BCS} from cavity measurements to find that increasing the concentration of dissolved O and N within the Nb metal will enhance performance. We can achieve similar improvements in Q_0 with either oxygen or nitrogen. However, there is an order of magnitude difference in the concentration of oxygen and nitrogen required to yield the same performance. A significantly lower concentration of nitrogen leads to the same reduction in R_{BCS} as oxygen. Nitrogen remains the most effective impurity for improving the Q_0 of SRF cavities.

ISBN: 978-3-95450-261-5 ISSN: 2673-7000 doi: 10.18429/JACoW-NAPAC2025-THYN01

REFERENCES

[1] D. Nueffer *et al.*, "An 8 GeV Linac As The Booster Replacement In The Fermilab Power Upgrade", arXiv, 2023. doi:10.48550/arXiv.2203.05052

[2] D. Bafia *et al.*, "Gradients of 50 MV/m in TESLA Shaped Cavities via Modified Low Temperature Bake", in *Proc. SRF'19*, Dresden, Germany, pp. 586–591, 2019. doi:10.18429/JACoW-SRF2019-TUP061

[3] H. Padamsee, J. Knobloch, and T. Hays, *RF Superconductivity for Accelerators*. Weinheim, Germany: Wiley-VCH GmbH, 1998.

[4] S. Isagawa, "Influence of hydrogen on superconducting niobium cavities", *J. Appl. Phys.*, vol. 51, pp. 6010–6017, 1980. doi:10.1063/1.327523

[5] J. Knobloch, "The 'Q disease' in Superconducting Niobium RF Cavities", in *First Int. Workshop on Hydrogen in Materials and Vacuum Systems*, vol. 671, pp. 130–150, 2003. doi:10.1063/1.1597364

[6] F. Barkov *et al.*, "Precipitation of Hydrides in High Purity Niobium after Different Treatments", *J. Appl. Phys.*, vol. 114, pp. 164904, 2013. doi:10.1063/1.4826901

[7] Y. Trenikhina *et al.*, "Nanostructural features degrading the performance of superconducting radio frequency niobium cavities revealed by transmission electron microscopy and electron energy loss spectroscopy", *J. Appl. Phys.*, vol. 117, 2015. doi:10.1063/1.4918272

[8] A. Grassellino *et al.*, "Nitrogen and argon doping of niobium for superconducting radio frequency cavities: a pathway to highly efficient accelerating structures", *Supercond. Sci. Tech.*, vol. 26, p. 102001, 2013. doi:10.1088/0953-2048/26/10/102001

[9] A. Grassellino *et al.*, "Unprecedented quality factors at accelerating gradients up to 45 MV/m in niobium superconducting resonators via low temperature nitrogen infusion", *Supercond. Sci. Tech.*, vol. 30, 2017. doi:10.1088/1361-6668/aa7afe

[10] A. Romanenko *et al.*, "Effect of mild baking on superconducting niobium cavities investigated by sequential nanoremoval", *Phys. Rev. ST Accel. Beams* vol. 16, pp. 012001, 2013. doi:10.1103/PhysRevSTAB.16.012001

[11] S. Posen *et al.*, "Ultralow surface resistance via vacuum heat treatment of superconducting radiofrequency cavities", *Phys. Rev. Applied*, vol. 13, p. 014024, 2020. doi:10.1103/PhysRevApplied.13.014024

[12] M. Martinello *et al.*, "Field-Enhanced Superconductivity in High-Frequency Niobium Accelerating Cavities", *Phys. Rev. Lett.*, vol. 121, p. 2248012018. doi:10.1103/physrevlett.121.224801

[13] B. P. Xiao, C. E. Reece, and M. J. Kelley, "Superconducting surface impedance under radiofrequency field", *Physica C*, vol. 490, pp. 26–31, 2013. doi:10.1016/j.physc.2013.04.003

[14] A. Gurevich, "Reduction of Dissipative Nonlinear Conductivity of Superconductors by Static and Microwave Magnetic Fields", *Phys. Rev. Lett.*, vol. 113, no. 8, p. 087001, 2014. doi:10.1103/physrevlett.113.087001

[15] G. Ciovati, P. Dhakal, and A. Gurevich, "Decrease of the surface resistance in superconducting niobium resonator cavities by the microwave field", *Appl. Phys. Lett.,* vol. 104, no. 9, p. 092601 2014. doi:10.1063/1.4867339

[16] D. C. Ford, L. D. Cooley, and D. N. Seidman, "First-principles calculations of niobium hydride formation in superconducting radio-frequency cavities", *Supercond. Sci. Technol.*, vol. 26, p. 095002, 2013. doi:10.1088/0953-2048/26/9/095002

[17] D. Bafia *et al.*, "The role of oxygen concentration in enabling high gradients in niobium SRF cavities", in *Proc. SRF'21*, East Lansing, MI, USA, Jun.–Jul. 2021. doi:10.18429/JACoW-SRF2021-THPTEV016

[18] E. M. Lechner *et al.*, "RF surface resistance tuning of superconducting niobium via thermal diffusion of native oxide", *Appl. Phys. Lett.*, vol. 119, p. 082601, 2021. doi:10.1063/5.0059464

[19] E. M. Lechner *et al.*, "Oxide dissolution and oxygen diffusion scenarios in niobium and implications on the Bean–Livingston barrier in superconducting cavities", *J. Appl. Phys.*, vol. 135, p. 133902, 2024. doi:10.1063/5.0191234

[20] D. Bafia, A. Grassellino, and A. Romanenko, "The Anomalous Resonant Frequency Variation of Microwave Superconducting Niobium Cavities Near T_c", arXiv, 2021. doi:10.48550/arXiv.2103.10601

[21] H. Hu, D. Bafia, and Y.-K. Kim, "Evaluating the Effects of Nitrogen Doping and Oxygen Doping on SRF Cavity Performance", in *Proc. IPAC'22*, Bangkok, Thailand, Jun. 2022. doi:10.18429/JACoW-IPAC2022-TUPOTK034

[22] P. N. Koufalis *et al.*, "Effects of Interstitial Oxygen and Carbon on Niobium Superconducting Cavities", arXiv, 2017. doi:10.48550/arXiv.1612.08291

[23] A. Budrevich and J. Hunter, "Metrology aspects of SIMS depth profiling for advanced ULSI processes", in *Characterization and Metrology for ULSI Technology*, vol. 449, pp. 169–181, 1998. doi:10.1063/1.56792